Uniform Linear Arrays with Hybrid Beamforming: To Overlap or Not To Overlap?

Margaux Pellet[1,2], George Goussetis[1], Joao Mota[1], Hervé Legay[2], Giovanni Toso[3], Piero Angeletti[3]
[1] Heriot-Watt University, Edinburgh, Scotland, mp2026@hw.ac.uk
[2] Thales Alenia Space, Toulouse, France, herve.legay@thalesaleniaspace.com
[3] European Space Research and Technology Centre, ESA-ESTEC, Noordwijk, the Netherlands, G.Toso@esa.int

***Abstract*—Overlapping strategies for hybrid beamformed direct radiating arrays have been studied in the past decades as a means to improve the gain of a directive beam. It is widely known that overlapping subarrays guarantees the suppression or the partial mitigation of some unwanted grating lobes. However, such techniques come with a cost, either in terms of hardware or in terms of digital complexity. Performance-wise, the overlapping strategies have also shown particular cases where the scanning improvements were not evident. This paper presents a study of the general overlapping principles in hybrid analogue-digital beamformed direct radiating arrays for the case of a GEO satellite application. This study allows to identify cases where the overlapping technique is beneficial compared to a non-overlapped array.**

Keywords—antenna arrays, beamforming, satellite antennae, space application, telecommunications

I. Introduction

Over the past years, with the transition from broadcast to broadband satellite communications, active direct radiating array antennas have been seen as a key solution to guarantee high performance in terms of capacity, flexibility and reconfigurability [1]. Such configuration gives a full flexibility in terms of coverage as beams can be steered along any desired direction within the field-of-view. However, the hardware complexity of such antenna configurations is unaffordable particularly in light of today's on-board processors that can process digitally up to a few hundreds of ports. In conjunction with hardware limitation for the solid-state amplifiers, the technological requirements lead to unrealistic architectures, especially for GEO coverages where thousands of radiating elements are needed.

Hybrid beamforming is introduced as a solution to reduce the antenna complexity [2,3]. Instead of having all the radiating elements connected to the on-board processor, the system is split into analogue beamformed subarrays which in turn are digitally processed. At the analogue level, radiating elements are processed within a subarray. In turn, the digital level performs the lattice of subarrays. This cascade of analogue beamforming (ABFN) and digital beamforming (DBFN) guarantees a reduction in the number of ports from thousands to dozens. In terms of coverage, the analogue device enables large regional beam generations, within which narrow spot beams are defined by the digital processor (Fig. 1.) [5].

However, this improvement in terms of complexity comes with drawbacks from a performance perspective. Indeed, subarrays are now seen as large radiating elements from the digital point-of-view. Grating lobes are generated: they are undesirable for the payload system as they correspond to interferences for multibeam antennas. To fulfil the grating lobe mitigation, several techniques have been explored in the literature such as sparsity [6] or polyominoes arrays [7, 8]. Another technique exploits overlapped subarrays [9-10].

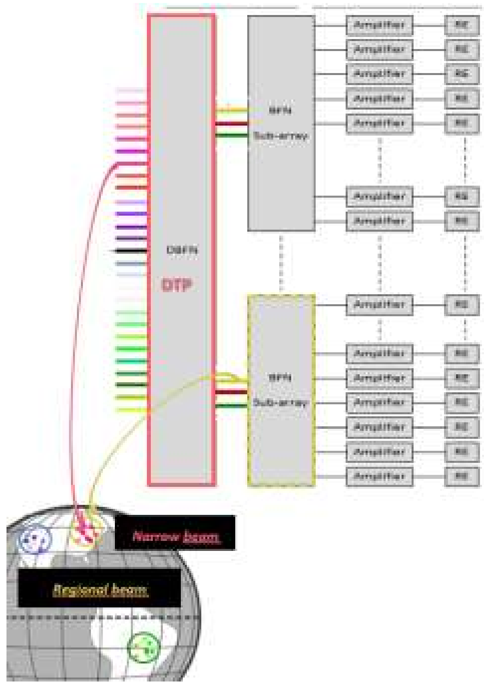

Fig. 1. : Hybrid beamforming scheme [5]

The latter technique enables to fully or partly suppress some grating lobes. In [9], each subarray is overlapped with the adjacent ones: the elements at the edges of the subarrays are fed by 2 subarrays. Although the technique is efficient when scanning close to nadir, this architecture relies on different types of active radiating elements along the array and at least two types of amplifiers are required to implement such an architecture. In [10], the subarrays are overlapped thanks to an interleaved layer of tiles shifted by half the size of a subarray along the two Cartesian axes directions. It permits to mitigate odd grating lobes and has a simple hardware scheme. However, the levels of even grating lobes are increased, additional subarrays are used, and the power normalisation must occur at element level to avoid power loss, which increases the digital complexity. In this contribution, a general case considering both periodic overlapping configurations is presented. The contribution is limited to radiating elements fed by at the maximum 2 subarrays to give a first approach of the general configuration. From this linear architecture, it is shown that, with an equivalent complexity, overlapping is not always beneficial.

II. Uniform Linear Array with Displacement of the Tiles toward the Centre of the Array

A. Technique definition

First, a non-overlapped linear array is defined with 6 subarrays each of 6 radiating elements, as shown in Fig. 2. For defining a general case, we revisit the concept of overlapped arrays. For all cases from [9] to [10], despite having very different visions on how to generate an overlap between subarrays, a common feature is observed. Centres of gravity for each subarray can be identified. It corresponds to the middle of them. Then, a sampling step is added such that the final centre of gravity considers the closest radiating element as the new centre. If it is situated in-between 2 radiating elements, the first one from the left side is chosen. Indeed, by identifying the centres of gravity of the subarrays, it is analysed that the main idea relies on the displacement of the tiles toward the centre of the overall array. Therefore, the general overlapping is defined as follows:

- The subarrays at the edge are extended by a controlled percentage of the size of a subarray
- The centres of gravity of the extended tiles/subarrays are retrieved.
- From these centres, the regularity between the other central centres of gravity is kept. These situated in-between are moved according to a division of the new total distance between the edge feeds by the number of subarrays.
- The subarrays are all extended by the same number of radiating elements. The tile related to each subarray is attached to it thanks to a sampling of the total array length.

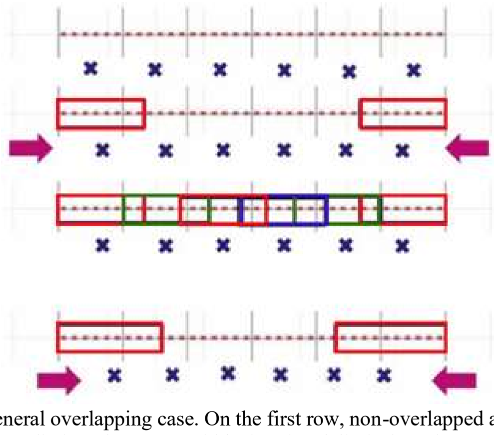

Fig. 2.: General overlapping case. On the first row, non-overlapped array. In red crosses radiating elements and black strips delimit the subarrays. In red crosses, radiating elements. On the second row, the subarray is extended. The rectangles indicate the size of a subarray. On the third row, the feeds are displaced and associated to each subarray. On the fourth row, an example with a larger extension is shown.

The full process is described in Fig.2. One of the main highlights is the proximity of the subarrays' centres compared to the non-overlapped array. Indeed, by extending the subarray the unit cell associated with the array periodicity is reduced. It is noted that, in the proposed case, extending the subarrays further implies a more significant displacement of the subarray centres toward the middle of the linear array. Another observation is that, because the array length is sampled by the number of tiles, the overlap between adjacent subarrays is aperiodic. Indeed, 2 radiating elements are fed by 2 subarrays at the edges while 3 of them are fed by 2 subarrays between the second and the third subarrays (Fig. 2. third row). On the contrary, in the case-study in [9], the overlapping between adjacent subarrays is periodic. This is due to a manufacturing correction. Indeed, implementing an array with feeds all situated at the centre of the tiles is simpler as the connections between radiating elements and subarrays are similar for all subarrays.

However, the theoretical idea behind [9] and the general overlapping is the same with extension of the inner tiles. Except adding a periodicity, the feeding network is similar. It is detailed in Fig. 3.

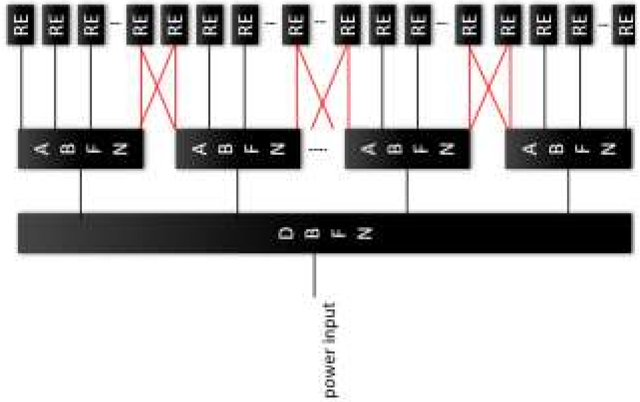

Fig. 2. : Feeding network of the general overlapped case

As shown, radiating elements at the edge of a tile are connected to the adjacent subarray's ABFN. The main differences between [9] and the general overlapping are the positions of the connections between the ABFNs and DBFN and the number of red connections between radiating elements. However, in such feeding network, the power is first normalized at each ABFN level, and then at DBFN such that the network is lossless. The phase between neighbour subarray is not in coherence, which leads to the need of an additional step of normalization at radiating element level. It is similar in both [9] and presented configurations.

B. Radiation pattern characteristics

According to the previously defined architecture, the radiation patterns are generated in Fig. 4. for a scan of the spot beam at $\theta = 1°$. The ABFN scanning is fixed at nadir and only a DBFN steering is considered. For all cases the power is uniformly distributed over the array. The overlap ratio indicated under each radiation pattern corresponds to the ratio of radiating elements added to each subarray. For instance 1/6 would be 1 radiating element added to the 6 from the inner tile. The maximum overlap considered here is ½, which means the subarrays are at the maximum overlapped with the adjacent subarrays, and there cannot be more than 2 overlapped subarrays.

As depicted, there is a displacement toward the end-of-coverage of the grating lobes. Indeed, if the grating lobe situated at $\theta = -5.5°$ $\theta = -5.5°$ is considered, it is observed that between 0 and 1/3 overlap, the grating lobe moves from to $\theta = -6°$ $G = -20$. However, its level is not necessarily attenuated: for instance, when comparing the 0 and ½ overlap cases, the same grating lobe gain is at dB. This displacement is due to the lattice associated with the periodicity. Indeed, having closer feeds implies farther grating lobe.

When considering the first order grating lobe at $\theta = -2.2°$, its level is reduced significantly the more the array is overlapped. Indeed, it goes from $G = 27.2$ dB without overlap to 26.4 dB for 1/6 , to finally end up at 20.3 dB for ½. The mitigation is due to the extension of the subarray. Indeed, changing the inner subarray has an impact on the subarray pattern: generating larger subarrays consequently produces a narrower subarray pattern. The null of the aforementioned pattern is therefore ideally positioned to isolate the first order grating lobe from the main beam.

In terms of grating lobes, it seems that there is an overall improvement. Nevertheless, this improvement seems dependent on the scanning position.

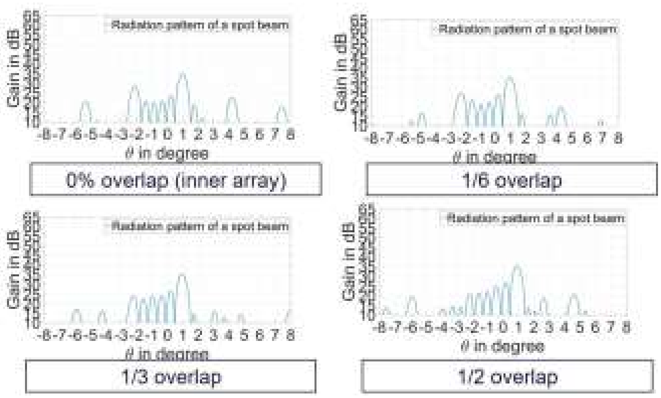

Fig. 3. : Radiation patterns simulated with different extension ratios

III. Extension of the General Overlapping to Drastically Closer Tiles Cases

A. *Further array characteristics*

The overlapping methodology presented in [10] can also be seen as a particular case compared to the one defined in this contribution. Since the transition from one case to the other is not straightforward, it is detailed in Fig.5. As immediately noticed, this case is an extension of the previous Section II where not more than 2 subarrays can feed a radiating element.

As depicted, the first change compared to the inner non-overlapped array is to consider feeds that are drastically closer. It implies subarrays significantly broadened because of the displacement of the centre of gravity due to the extension. It is illustrated with the second row. On the third row, it is observed that, by superimposing the extended subarrays associated with all the feeds, there are areas within the linear array for which radiating elements are fed by several subarrays. Here, these areas are shown for feeds that are twice closer than the inner ones. When comparing these areas with the inner subarray length, it corresponds to twice smaller subarrays. However, there are different lengths associated with the aforementioned portions. On the fourth row, missing tiles are added to limit bore-effect. The overall number of subarrays is doubled. The number of subarrays between subarrays intersections is the same across the array: here, it corresponds to 3 radiating elements. Nevertheless, it is worth mentioning that these 3 radiating elements are not fed by an equal number of subarrays. For instance, at the edges there are 8 subarrays per radiating elements while at the centre there are 12. The interest of overlapping is that subarrays that are not in phase coherence feed the same radiating elements. A constraint given for the general overlapping definition is to ensure each radiating element is fed by at the maximum 2 subarrays. To achieve so, the subarrays are truncated around the centre of gravity. All subarrays are therefore the same length and the hardware complexity is managed by replicating the same devices across the architecture.

The architecture from [10] is a particular case as there is exactly twice closer subarrays compared to the inner non-overlapped array. This is also the case illustrated in Fig. 5. Because the subarrays are truncated such that they cannot cover more than another subarray, their length is exactly equal to the ones from the inner array.

In terms of the feeding network, the principle is the same as in Fig. 3., considering that ABFN are introduced in cascades. It is worth mentioning that in terms of digital complexity, adding subarrays is synonymous with adding digital controls to the DTP.

As a summary, the general overlapping case is the following: the tiles are displaced toward the centre of the linear array thanks to the extension of subarrays. If the subarrays are superimposed more than twice, then they are equally cut and tiles are added to avoid bore-effects (Fig. 5.). Otherwise, they are unchanged and do not require any additional feed (Fig. 2.).

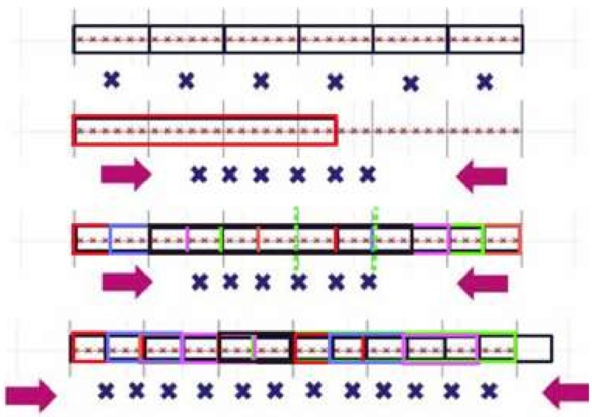
Fig. 4. : General overlapping case. On the first row, non-overlapped. On the second row, displacement of the tiles toward the centre with subarrays highly extended. On the third row, superposition of subarrays from all the tiles. In green dot lines; the green subarray is truncated to prevent elements fed by more than 2 subarrays. On the fourth row, additional tiles are added to cover the edges and truncation applied to all subarrays.

B. *Radiation pattern characteristics*

The radiation pattern of the general overlapped configuration with additional DCs is given in Fig. 6. for a scan at $\theta = 1°$. It is noted that the configuration has subarrays of 36 radiating elements. For the inner array, the architecture corresponds to 6 subarrays. For the overlapped with a 1/6 offset, it means 1 element is fed by two subarrays and 5 are fed by only one. It adds 1 subarray. For the half offset, there are 6 additional subarrays. The purpose here is to see if, for a uniform power distribution across the linear arrays, there is any improvement in terms of grating lobe mitigation.

For the 1/6 offset. There is a slight tapering effect on the grating lobes. The same phenomenon of grating lobe displacement occurs as per the case 1/6 from Fig. 4, which is related to similar overlaps. This case acts as a justification that both overlapping cases from the literature can be generalized by the proposed case of tile displacement.

When comparing the inner array with the half offset case, it is worth noting that all the odd grating lobes are suppressed. This is of strong added value in terms of interference. However, the inner array has twice less DCs. If a non-overlapped array with a same number of DCs is considered, and hence has twice smaller subarrays to keep the same radiating aperture, the radiation patterns are exactly the same between the overlapped and the non-overlapped configurations.

When the tiles are displaced toward the centre of the array, it is possible to totally mitigate some grating lobes at the condition of having tiles situated twice closer than for the inner array. This is due to the non-coherence of phase. The perfect phase opposition between adjacent subarrays occurs for a perfect superimposition of them of half the size of a subarray. However, displacing the tiles a bit less does not prevent from grating lobes and simply adds a digital complexity. The only option for tiles drastically moved toward the centre is therefore to have twice closer tiles than the inner configuration.

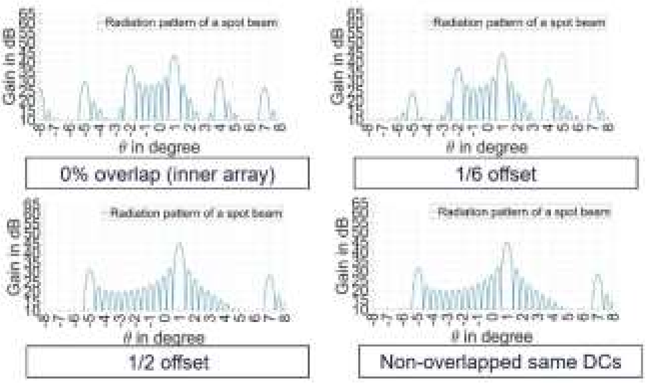

Fig. 5. : radiation patterns with different number of tiles added to the array due to the extensive overlap.

IV. SCAN LOSS DISCUSSION

An important objective is to improve the scanning performances. For satellite communications a high gain within a defined area is required. This area can also be broadened to reduce the complexity further. The idea in this section is to exploit the observations made from the two defined cases of the general overlapping. From these depictions, the overlapping parameters can be studied. The first processed case is the one from section II. The purpose is to define in which cases, if any, there is an improvement compared to the non-overlapped case.

To achieve such comparison, the main beam at DBFN level is scanned within the regional ABFN beam from nadir. The angle is increased every θ θ 0. 01° . For every iteration of , the main beam is scanned. A threshold is set called the ½ power threshold. It corresponds to the gain with the maximum radiating aperture minus 3 dB. Beyond this value, more than half of the power is taken from the main beam by interfering grating lobes. The area within which it is reasonable scanning is therefore between the maximum achievable gain and the threshold, and is referred to as "scanning range" in the following. In the study, no feeds are added, i.e., the general case where subarrays are at best overlapped once is considered. Indeed, it has been shown that there is no added value adding tiles in terms of grating lobe mitigation except when the tiles are twice closer. This case is explored later.

The results are presented in Fig. 7. The uniform taper is preserved such that all the radiating elements are fed with exactly the same power. The tapering effect is discussed in the following, but a first study is led on the degree of overlapping.

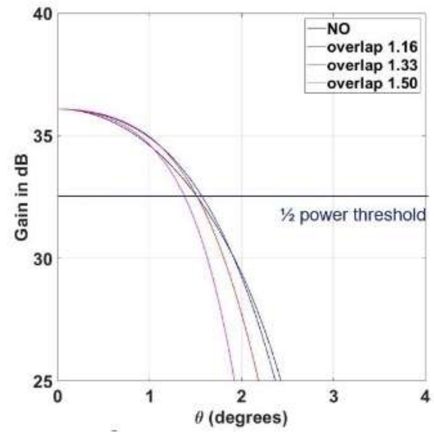

Fig. 6. : Scan loss from nadir for the non-overlapped array (NO) and different extension ratio for the overlapping configuration

As observed, the non-overlapped (NO) configuration is not always the worst case scenario. Indeed, in terms of scanning range, there is a slight decrease of 0.21° between NO and an overlap of 1.50 (corresponding to ½ overlap from Fig. 3). As depicted, the null of the regional beam situated at 2.0° enforces a drastic decrease of the gain. It is worth noting that, before the curves reach the threshold, the gain is more constant for the 1.5 overlap case than for the NO configuration. Moving to 1.16 overlap, the scanning range is also more constant. The gain between nadir and the threshold is increased by 1.17 dB overall and the scanning range is improved by 0.05°. In the 1.33 case, however, the improvement is less noticeable in terms of gain while not guaranteeing any increase of the scanning range. Indeed, the gain is increased by 0.98 dB. It seems that, by ensuring a uniform power distribution all over the array, there is no improvement guaranteed by overlapping due to the position of the first null of the subarray pattern that is set closer. Indeed, adding connections between radiating elements and ABFNs is a hardware complexity. The decision then rests with the system designers as to whether a 1dB-order gain improvement worth this additional complexity in a mission context.

The position of these nulls can nevertheless be changed thanks to a tapering at ABFN level. Indeed, a broadening of the subarray pattern main lobe is performed thanks to Gaussian-shaped tapers (e.g. Taylor, dB tapers, or Hamming window). In particular, the contribution focuses on the parameterization of such tapers. The targeted investigation is whether a taper can improve the scanning range and if so, define the specific cases for which it is worth overlapping.

To achieve such investigation, a Hamming Window is applied at each subarray level. In (1), x_k denotes the position of the radiating elements within a non-steered subarray.

$$w(k) = \alpha + (1-\alpha)\cos(2\pi x_k) \tag{1}$$

The $\alpha \in [0\ 1]$ parameter can vary and therefore generate several types of tapers with different heights of pedestal. When α is close to 1, the taper is almost uniform. When α is very low, the taper is a full Gaussian. The effect of the taper itself can be extracted with the use of the general case when tiles are twice closer than the non-uniform case. This case is presented on Fig. 8. As depicted, α varies from 0.4 to 0.7 by steps of 0.02.

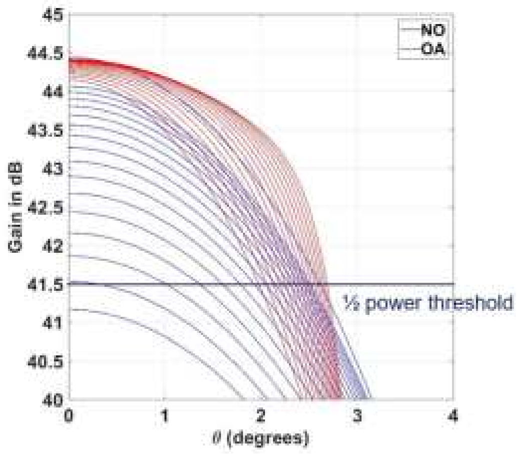

Fig. 7. : Tapering impact on the scan losses. Comparison between the overlapped configuration (OA) and the NO one

For the NO case, the higher the α, the better the scanning range and the gain within the scanning area. The highest gain is performed by a uniform taper with $\alpha = 1$ and is set as a reference for the comparison. For this value, NO and OA (overlapped arrays) are fully superimposed as already suggested by the radiation patterns from Fig. 6.

A first observation is that tapering does not guarantee an improvement with overlapped subarrays. Indeed, when α is low, i.e., for α between 0.4 and 0.48 or very high between 0.62 and 0.70, there is no added value using a taper. It even decreases the performances given by OA. Both gain and scanning range are degraded. Between 0.48 and 0.62 , there is always a gain improvement compared to the uniform taper. However, only a range in [0.52 0.58] guarantees a better scanning range and gain. For $\alpha = 0.56$ there is an optimal gain reached as well as the best scanning range. It leads to a gain improvement of 2.5 dB and an extended scanning area by 0.16°.

By applying a similar study to the general case limited to extended subarrays and no tile addition, the improvements are similar but with different parameters depending on the extension.

V. Conclusion

A general overlapping technique for linear arrays has been studied where the contribution is limited by two subarrays per radiating elements. Such technique enable an investigation on either it is worth overlapping subarrays. By displacing the tiles of the subarrays, it is possible to show for several periodic overlapping cases from the literature that overlapping is not always beneficial. A strong tapering study is needed to find the optimal improvement in terms of gain. Depending on the type of application, the taper choice must be done wisely considering the hardware cost of such technique.

Acknowledgment

This work has been supported by the European Space Agency under contract No. 4000135641/21/NL/GLC/my

References

[1] R. De Gaudenzi, P. Angeletti, D. Petrolati and E. Re, “Future technologies for very high throughput satellite systems,” *Wiley Int. Journ. of Satellite Communications and Networking*, Vol. 38, No. 2, pp. 141-161, Mar./Apr. 2020, doi:10.1002/sat.1327

[2] P. Angeletti, G. Toso, D. Petrolati, ‘A reconfigurable multibeam antenna system’ European Patent EP 3 654 544 A1, filing date: 13-11-2018.

[3] S. J. Stirland, and A. D. Craig. “Phased arrays for satellite communications: Recent developments at astrium LTD,” In *The Second European Conference on Antennas and Propagation, EuCAP 2007*, pp. 1-5. IET, 2007.

[4] R. Palisetty *et al*., "Area-Power Analysis of FFT Based Digital Beamforming for GEO, MEO, and LEO Scenarios," *2022 IEEE 95th Vehicular Technology Conference: (VTC2022-Spring)*, Helsinki, Finland, 2022, pp. 1-5, doi: 10.1109/VTC2022-Spring54318.2022.9861037.

[5] M. Pellet, G. Goussetis, H. Legay, J. Mota, G. Toso and P. Angeletti, “ Hybrid Beamformed Direct Radiating KA-Band Arrays for Multibeam Coverage with Frequency Reuse” 41th esa antenna workshop, 2023

[6] M. C. Viganó, G. Toso, G. Caille, C. Mangenot, and I. E. Lager. “Sunflower array antenna with adjustable density taper”, *International Journal of Antennas and Propagation*, 2009.

[7] R. J. Mailloux, S. G. Santarelli, T. M. Roberts, and D. Luu, “Irregular Polyomino-Shaped Subarrays for Space-Based Active Arrays,” *Int J Antennas Propag*, vol. 956524, 2009, doi: 10.1155/2009/956524

[8] P. Rocca, R. J. Mailloux, and G. Toso, “GA-based optimization of irregular subarray layouts for wideband phased arrays design”, *IEEE Antennas and Wireless Propagation Letters* Vol. 14, pp. 131-134, 2014.

[9] V. Tugend and A. Thain, “Hybrid beamforming with reduced grating lobes for satellite applications,” *12th European Conference on Antennas and Propagation (EuCAP 2018),* p 1-5, 2018.

[10] M. Pellet, G. Goussetis, H. Legay, J. Mota, B. Cortazar, and G. Toso, “A new antenna array architecture with hybrid beamforming for broadband satellite communications” *17th European Conference on Antennas and Propagation (EuCAP 2023)*, 2023